J Therm Anal Calorim (2009) 98:731–736
DOI 10.1007/s10973-009-0105-5

# Crystallization kinetics of $SrBi_2B_2O_7$ glasses by non-isothermal methods

**Koushik Majhi · K. B. R. Varma**

Received: 14 November 2008 / Accepted: 17 February 2009 / Published online: 23 June 2009


**Abstract** Transparent glasses of $SrBi_2B_2O_7$ (SBBO) were fabricated via the conventional melt-quenching technique. The amorphous and the glassy nature of the as-quenched samples were, respectively, confirmed by X-ray powder diffraction (XRD) and differential scanning calorimetry (DSC). The glass transition ($T_g$) and the crystallization parameters [crystallization activation energy ($E_{cr}$) and Avrami exponent ($n$)] were evaluated under non-isothermal conditions using DSC. There was a close agreement between the activation energies for the crystallization process determined by Augis and Bennet and Kissinger methods. The variation of local activation energy [$E_c(x)$] that was determined by Ozawa method, decreased with the fraction of crystallization ($x$). The Avrami exponent ($n(x)$) increased with the increase in fraction of crystallization ($x$) suggesting that there was a change over in the crystallization process from the surface to the bulk.

**Keywords** Glass transition · Crystallization · Borate · Non-linear optics · Polar · Activation energy

## Introduction

Glasses comprising non-linear optical crystals have been of increasing interest for a variety of applications. For instance, transparent crystallized glasses of $LaBGeO_5$, $SrBi_2Ta_2O_9$, $SrBi_2Nb_2O_9$, which are important from their multi-functionalities view point have been fabricated and characterized [1–3]. Recently $SrBi_2B_2O_7$ (SBBO) was reported to be belonging to hexagonal crystal system associated with $P6_3$ polar space group [4]. Since it is polar, we thought it is worth fabricating transparent-glasses of SBBO embedded with nano/microcrystallites of the same composition and examine their physical properties as these composites have great potential for device applications. To begin with, we aimed at understanding the crystallization kinetics as these provide a priori knowledge about optimization of certain parameters that are important in the fabrication of optical glass nano/micro crystal composites.

Differential thermal analysis (DTA) and differential scanning calorimetry (DSC) could frequently be used to study the crystallization kinetics of the glassy materials [5–9]. For determining the kinetic parameters such as the activation energy of crystallization ($E_{cr}$) and Avrami exponent ($n$) in Johnson–Mehl–Avrami (JMA) equation [10–12], for the present SBBO glasses, non-isothermal methods are employed. The activation energy associated with the crystallization is determined using Kissinger [13] and Augis and Bennet [14] methods. Heating rate dependent crystallization temperature is rationalized using Lascoka equation [15]. Also the variations of activation energy and Avrami exponent with the fraction of crystallization are examined. The details of which are reported in this paper.

## Experimental

SBBO glasses were fabricated via the conventional melt-quenching technique. For this, $SrCO_3$ (99.95%, Aldrich); $Bi_2O_3$ (99.9%, Merck); and $B_2O_3$ (99.9%, Aldrich) were mixed and melted in a platinum crucible at 1373 K for 1 h. Melts were quenched by pouring on a steel plate and pressed with another plate to obtain 1–1.5-mm thick glass

K. Majhi · K. B. R. Varma (✉)
Materials Research Centre, Indian Institute of Science, Bangalore 560 012, India
e-mail: kbrvarma@mrc.iisc.ernet.in

plates. The DSC (Model: Diamond DSC, Perkin-Elmer) runs were carried out in the 550–800 K temperature range. For non-isothermal experiments, the glass samples were heated from 725 to 810 K (which covers the crystallization temperature) at different heating rates (5, 10, 15, 20, and 25 K/min). All the experiments were conducted in dry nitrogen ambience. The as-quenched glass-plates weighing 15 mg were used for all the experiments.

## Results and discussion

The X-ray diffraction pattern obtained for the as-quenched SBBO glass-plate is shown in Fig. 1. This pattern reveals the overall amorphous nature of the as-quenched sample. Inset in Fig. 1 shows the typical DSC trace recorded for the as-quenched SBBO glass-plate at a heating rate of 10 K/min. An endotherm around 670 K followed by an exotherm at 730 K associated with the glass transition ($T_g$), and the onset of the crystallization temperatures ($T_{cr}$), respectively, for the as-quenched sample are observed. The peak glass transition temperature ($T_p$) is the temperature at which it attains a maximum in the DSC curve (Fig. 1).

### Crystallization kinetics

Kinetic parameters [crystallization activation energy ($E_{cr}$) and Avrami exponent ($n$)] related to the glass crystallization process could be obtained from non-isothermal methods employing DSC experiments. Figure 2 shows the DSC traces (exothermic) obtained for the as-quenched SBBO glass-plates at different heating rates (5, 10, 15, 20, and 25 K/min). There is a systematic shift in the peak crystallization temperature ($T_p$) towards higher temperature with the increase in heating rates. Thus by monitoring the shift in the position of the exotherm as a function of the heating rate, one could obtain the kinetic parameters.

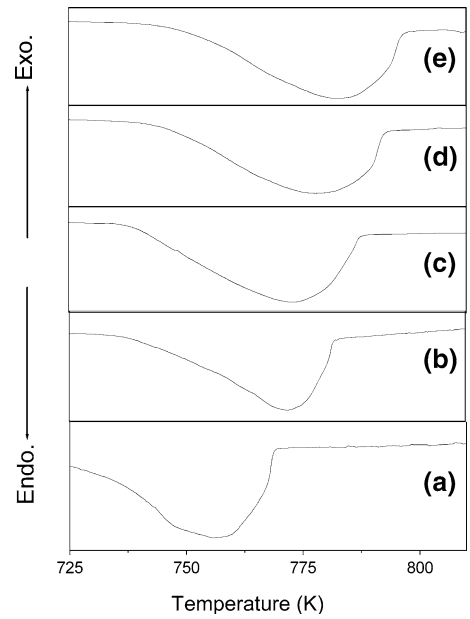


**Fig. 2** DSC traces for SBBO glass plate at various heating rates (*a*) 5 K/min, (*b*) 10 K/min, (*c*) 15 K/min, (*d*) 20 K/min and (*e*) 25 K/min

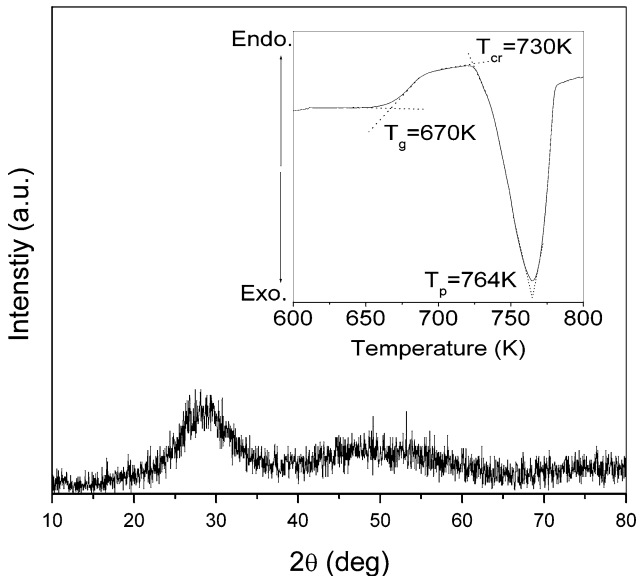


**Fig. 1** XRD pattern for the as-quenched $SrBi_2B_2O_7$ (SBBO) glass-plate; inset shows the DSC trace for the as-quenched $SrBi_2B_2O_7$ (SBBO) glass-plate

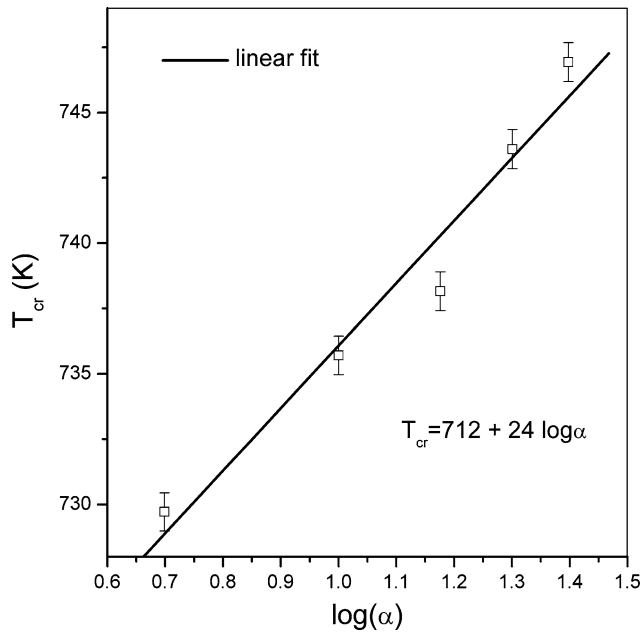


**Fig. 3** $T_{cr}$ versus log α plots for as-quenched plate SBBO glass samples

For rationalizing heating rate dependent crystallization temperature, Lasocka [15] equation can be invoked, which is stated as

$$T_{cr} = A_{cr} + B_{cr} \log \alpha \quad (1)$$

where $A_{cr}$ is the crystallization temperature at a heating rate of 1 K/min and $B_{cr}$ is a constant. Figure 3 shows the plot between $T_{cr}$ and log $\alpha$ (solid line is a linear fit) for the as-quenched SBBO glass-plate. The above relation for SBBO glasses could be written as

$$T_{cr} = 712 + 24 \log \alpha \quad (2)$$

The above equation is the effective description of the dependence of $T_{cr}$ on the heating rate for the as-quenched SBBO glasses.

The second approach that is adopted to analyze the $T_{cr}$ is non-isothermal crystallization kinetics for the as-quenched SBBO glasses. Most techniques, developed to study the crystallization kinetics based on the JMA equation [10–12] are essentially derived on the basis of experiments carried out under the isothermal conditions.

To understand the nucleation and growth process under the non-isothermal crystallization kinetics several theoretical methods [16] have been adopted based on the JMA equation. All the methods assume a constant heating rate, $\alpha$, in the DTA or DSC experiments, in which

$$T = T_0 + \alpha t \quad (3)$$

where $T_0$ is the initial temperature (300 K), $\alpha$ is the heating rate and $T$ is the temperature after time $t$. Primary goal of these methods was to identify two parameters, the overall effective activation energy, $E_{cr}$ and the order of the reaction or Avrami exponent, $n$.

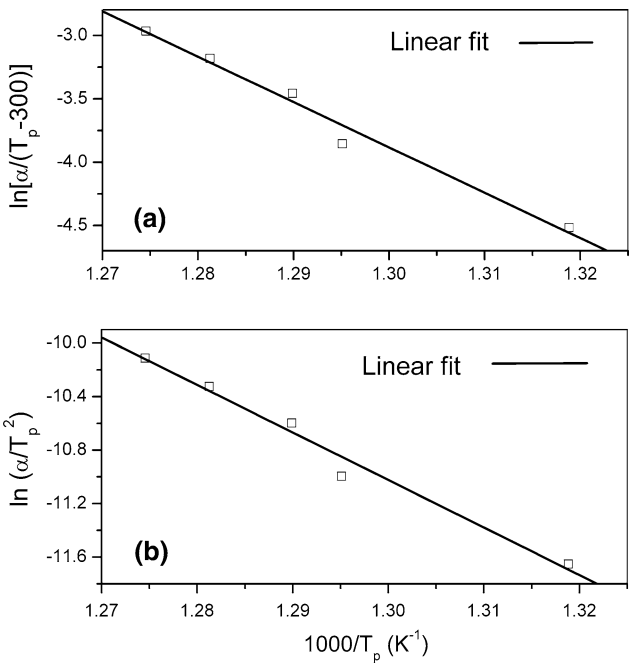


**Fig. 4** Plots of (**a**) $\ln[\alpha/(T_p - 300)]$ and (**b**) $\ln(\alpha/T_p^2)$ versus $1000/T_p$ for the SBBO glass

*Determination of the crystallization activation energy*

The crystallization activation energy could be extracted using the formula proposed by Augis and Bennet [14] as follows

$$\ln\left[\frac{\alpha}{T_p - T_o}\right] = \text{const.} - \frac{E_{cr}}{RT_p} \quad (4)$$

when $\ln[\alpha/(T_p - 300)]$ is plotted against $1/T_p$ (Fig. 4a), a straight line is obtained with a slope $-E_{cr}/R$. The value of $E_{cr}$ obtained for the as-quenched SBBO glass by this method is 297 ± 5 kJ/mol.

Kissinger [13] formulated the method that is commonly used for analyzing crystallization data in DSC or DTA experiments, according to which,

$$\ln\left(\frac{\alpha}{T_p^2}\right) = \frac{-E_{cr}}{RT_p} + \text{const.} \quad (5)$$

Figure 4b shows the plot of $\ln\left(\alpha/T_p^2\right)$ versus $1000/T_p$. The value obtained for $E_{cr}$ is 295 ± 5 kJ/mol, which is in close agreement with the value obtained by Augis and Bennet method.

It is observed that the crystallization peaks are asymmetric in nature (Fig. 2) for the as-quenched SBBO glasses under study. This implies that more than one process is active in the crystallization. Thus, to study the nature of the crystallization process, the fraction of crystallization ($x$) was determined. The fraction of crystallization ($x$) of the as-quenched glass during heating process could be obtained from the DSC data as a function of temperature ($T$) [17]. The fraction of crystallization ($x$), at any temperature $T$ is given by $x = (A_x/A)$, where $A$ is the total area under the exotherm between the temperature $T_i$, where the crystallization has just started and the temperature $T_f$, where the crystallization is completed, and $A_x$ is the area between the initial temperature and a temperature, $T$, ranging from $T_i$ to $T_f$.

Using the above technique, the fraction of crystallizations ($x$) was determined at different temperatures and heating rates for the as-quenched SBBO glasses. Figure 5a shows the typical sigmoidal curves for the fraction of crystallization ($x$) and temperatures ($T$) at various heating rates (5, 10, 15, 20, and 25 K/min). To determine the value of Avrami exponent ($n$), $\ln[-\ln(1 - x)]$ and $1000/T$ at different heating rates were plotted. Figure 5b shows the plots of $\ln[-\ln(1 - x)]$ and $1000/T$ at different heating rates. It is noticed that in the entire range of temperatures, the plots are non-linear at all the heating rates under study.

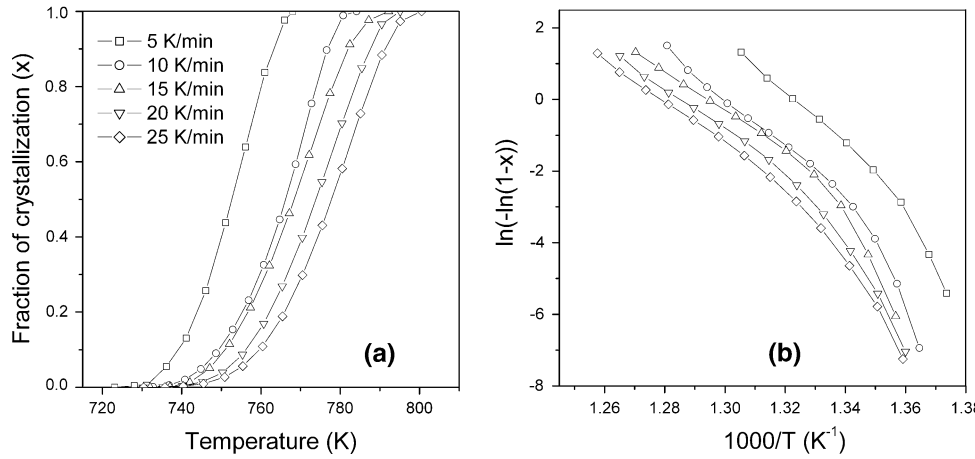


**Fig. 5** (**a**) Fraction of crystallization versus temperature curves at various heating rates for SBBO glass-plates, (**b**) plot of $\ln[-\ln(1-x)]$ versus $1000/T$ for the SBBO glass plate at various heating rates

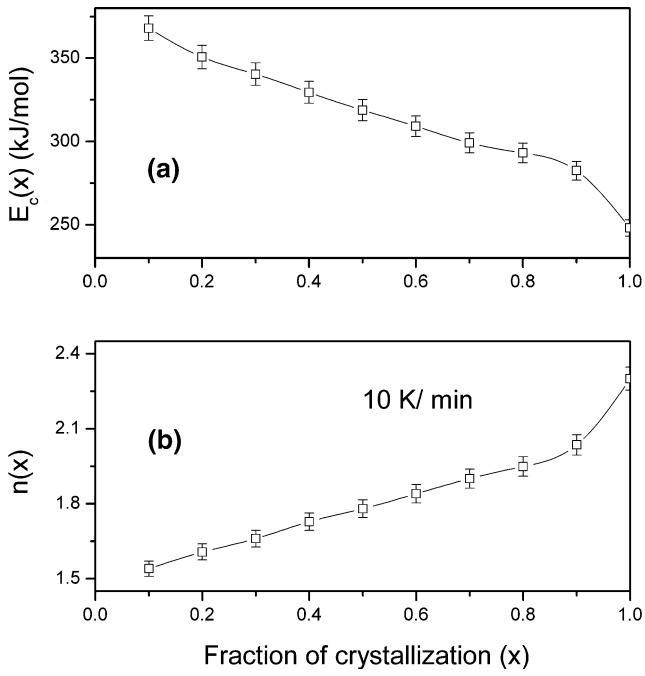


**Fig. 6** (**a**) $E_c(x)$ and (**b**) the local Avrami exponent $n(x)$ as a function of crystallized fraction ($x$) (at a 10 K/min heating rate) for the SBBO glass

According to the modified Ozawa equation [18], the fraction of crystallization ($x$) and the temperature ($T$) for the as-quenched glasses could be related as

$$\ln[-\ln(1-x)] = -n\ln\alpha - 1.052(n-1)\frac{E_{cr}}{RT} + \text{const.} \quad (6)$$

where $E_{cr}$ is the activation energy for the crystallization, $n$ is the Avrami exponent, $T$ is the temperature in absolute scale, $R$ is the universal gas constant. From the above equation, the plot of $\ln[-\ln(1-x)]$ and $1000/T$ should be straight line with the slope $1.052(n-1)E_{cr}/R$, but in the present study these trends are found to be non-linear as shown in Fig. 5b at all the heating rates. It suggests that there is a variation in $E_{cr}$ and $n$ during crystallization process of SBBO glass-plates. In the above context it is interesting to study the change in the activation energy and Avrami exponent during the crystallization of SBBO glasses.

*Local activation energy*

Generally, the activation energy is defined as the threshold energy above which the fluctuation of energy in the activation complex is sufficient for the elementary reaction to take place. The value of the activation energy is constant and characteristic for each reaction. It is observed that in few glass systems, the activation energy is dependent on the fraction of crystallization [19–21]. So, a local activation energy $E_c(x)$, which represents the activation energy at a stage when the crystallized volume fraction is $x$, is applied to describe the variable activation energy which reflects the change of nucleation and growth behavior during crystallization process.

The calculation of the local activation energy $E_c(x)$ could be obtained using non-isothermal DSC experiments. The local activation energy $[E_c(x)]$ for the crystallization of the as-quenched SBBO glass-plates is determined using the method introduced by Ozawa [22]. According to which

$$\left[\frac{\mathrm{d}\ln\alpha}{\mathrm{d}(1/T)}\right]_x = -\frac{E_{cr}(x)}{R} \quad (7)$$

where, $R$ is gas constant, $T$ and $\alpha$ are the temperature and the heating rate corresponding to the value of $x$.

Using the experimental data that are depicted in Fig. 5a, $\ln\alpha$ and $1/T$ is plotted at various values of $x$ and the $E_{cr}(x)$ is obtained from the slope of the curve. Figure 6a shows the variation of the crystallized volume fraction and the local activation energy for the as-quenched SBBO glass-plate. It is noticed that at the initial stages of crystallization process, the local activation energy of the crystallization of the as-quenched SBBO glass is $368 \pm 5$ kJ/mol ($x = 0.1$).

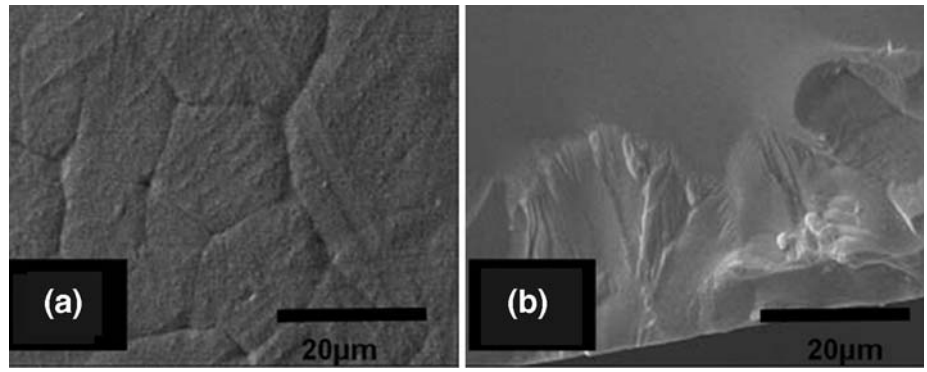


**Fig. 7** Scanning electron micrographs of the SBBO heat-treated (670 K/12 h) glasses (**a**) top view of the crystallized surface and (**b**) cross-sectional view of crystallized surface

When the crystallized volume fraction is in the range of 0.3–0.8, the local activation energy decreases slowly. Beyond this point the local activation energy decreases rapidly with the fraction of crystallization ($x$).

It is known that the local activation energy [$E_c(x)$] is composed of two parts: activation energy associated with the nucleation ($E_n$) and the activation energy related to the growth ($E_g$) [23]. This could be expressed as:

$$E_c(x) = aE_n + bE_g \tag{8}$$

where $a$ and $b$ are two variables related to the Avrami parameter and $a + b = 1$. It is expected that at the beginning, the process of nucleation dominates ($b = 0$) and at the end of the crystallization, only the growth process ($a = 0$) is expected to dominate. As $x \to 0$, $E_c(x) \to E_n \approx 368 \pm 5$ kJ/mol and as $x \to 1$, $E_c(x)$ $E_g \approx 248 \pm 5$ kJ/mol for the present glasses.

*Avrami exponent*

According to Lu et al. [20] the expression to calculate Avrami exponent [$n(x)$] from the prior knowledge of local activation energy for non-isothermal crystallization process is,

$$n(x) = \frac{-R\partial \ln[-\ln(1-x)]}{E_c(x)\partial \ln(1/T)} \tag{9}$$

Taking into account the local activation energy [$E_c(x)$], Avrami exponents [$n(x)$] at a heating rate of 10 K/min were calculated using the above equation (Eq. 9) for the as-quenched SBBO glasses. Figure 6b shows the variation of Avrami exponent with the fraction of crystallization ($x$) at a heating rate of 10 K/min. The Avrami exponent increases from 1.5 to 2.3 which indicates that the crystallization process changes from the surface to two-dimensional bulk crystallization [20].

The surface and the cross-sectional SEM micrographs of the heat-treated (670 K/12 h) samples are shown in Fig. 7a and b, respectively. The micrograph shows well crystallized surface with closely packed grains (5–12 μm sized). However, the cross-sectional SEM micrograph reveals the surface crystallization layer thickness to be about 30–40 μm. It also clearly exhibits the presence of well defined growth fronts with the crystallites growing towards the bulk of the sample from the surface. Indeed these results corroborate the data obtained by crystallization kinetic studies.

## Conclusions

The crystallization parameters of SBBO glasses, which are scientifically important, have been evaluated using different methods derived from non-isothermal experiments. The average value of the crystallization activation energy is 297 ± 5 kJ/mol for sBBO glass-plates. The local activation energy for the as-quenched SBBO glasses is determined and found to be varying with the fraction of crystallization ($x$). The activation energies for the nucleation and growth processes are calculated and found to be 368 ± 5 and 248 ± 5 kJ/mol, respectively. The crystallization process in SBBO glasses could be either confined to surface or bulk, depending on the amount of fraction of the crystallization.

## References

1. Takahashi Y, Benino Y, Fujiwara T, Komatsu T. Second harmonic generation in transparent surface crystallized glasses with stillwellite-type $LaBGeO_5$. J Appl Phys. 2001;89:5282–7.
2. Murugan GS, Varma KBR, Takahashi Y, Komatsu T. Nonlinear-optic and ferroelectric behavior of lithium borate–strontium bismuth tantalate glass–ceramic composite. Appl Phys Lett. 2001;78:4019–21.
3. Prasad NS, Varma KBR, Takahashi Y, Benino Y, Fujiwara T, Komatsu T. Evolution and characterization of fluorite-like nano-$SrBi_2Nb_2O_9$ phase in the $SrO–Bi_2O_3–Nb_2O_5–Li_2B_4O_7$ glass system. J Solid State Chem. 2003;173:209–15.
4. Barbier J, Cranswick LMD. The non-centrosymmetric borate oxides, $MBi_2B_2O_7$ (M=Ca, Sr). J Solid State Chem. 2006;179:3958–64.

5. Ray CS, Zang T, Reis ST, Brow RK. Determining kinetic parameters for isothermal crystallization of glasses. J Am Ceram Soc. 2007;90:769–73.
6. Kissinger HE. Reaction kinetics in differential thermal analysis. Anal Chem. 1957;29:1702–6.
7. Mehta N, Kumar A. Comparative analysis of calorimetric studies in $Se_{90}M_{10}$ (M=In, Te, Sb) chalcogenide glasses. J Therm Anal Calorim. 2007;87:345–50.
8. Sánchez-Jiménez PE, Criado JM, Pérez-Maqueda LA. Kissinger kinetic analysis of data obtained under different heating schedules. J Therm Anal Calorim. 2008;94:427–32.
9. Nitsch K, Rodová M. Crystallization study of Na–Gd phosphate glass using non-isothermal DTA. J Therm Anal Calorim. 2008;91:137–40.
10. Avrami MJ. Kinetics of phase change. I. General theory. J Chem Phys. 1939;7:1103–12.
11. Avrami MJ. Kinetics of phase change. II. Transformation-time relations for random distribution of nuclei. J Chem Phys. 1940;8:212–24.
12. Avrami MJ. Granulation phase change, and microstructure kinetics of phase change. III. J Chem Phys. 1941;9:177–84.
13. Kissinger HE. Variation of peak temperature with heating rate in differential thermal analysis. J Res Nat Bur Stand. 1956;57:217–21.
14. Augis JA, Bennett JE. Calculation of the Avrami parameters for heterogeneous solid state reactions using a modification of the Kissinger method. J Therm Anal. 1978;13:283–92.
15. Lasocka M. The effect of scanning rate on glass transition temperature of splat-cooled $Te_{85}Ge_{15}$. Mater Sci Eng. 1976;23:173–7.
16. Bansal NP, Doremus RH, Bruce AJ, Moynihan CT. Kinetics of crystallization of $ZrF_4$–$Ba_2$–$LaF_3$ glass by differential scanning calorimetry. J Am Ceram Soc. 1983;66:233–8.
17. Prasad NS, Varma KBR. Crystallization kinetics of the $LiBO_2$–$Nb_2O_5$ glass using differential thermal analysis. J Am Ceram Soc. 2005;88:357–61.
18. Matusita K, Komatsu T, Yokota R. Kinetics of non-isothermal crystallization process and activation energy for crystal growth in amorphous materials. J Mat Sci. 1984;19:291–6.
19. Calka A, Radlinski AP. The local value of the avrami exponent: a new approach to devitrification of glassy metallic ribbons. Mater Sci Eng. 1988;97:241–6.
20. Lu W, Yan B, Huang W. Complex primary crystallization kinetics of amorphus Finemet alloy. J Non Cryst Solids. 2005;351:3320–4.
21. Lu K, Wang JT. Activation energies for crystal nucleation and growth in amorphous alloys. Mater Sci Eng A. 1991;133:500–3.
22. Ozawa T. Applicability of Friedman plot. J Therm Anal. 1986;31:547–51.
23. Yinnon H, Uhlmann DR. Applications of thermoanalytical techniques to the study of crystallization kinetics in glass-forming liquids, part I: theory. J Non Cryst Solids. 1983;54:253–75.